



## Crossover from negative to positive magnetoresistance in a Si delta-doped GaAs single quantum well

Shun-Tsung Lo<sup>a</sup>, Kuang Yao Chen<sup>a</sup>, Yi-Chun Su<sup>a</sup>, C.-T. Liang<sup>a,\*</sup>, Y.H. Chang<sup>a</sup>, Gil-Ho Kim<sup>b</sup>, J.-Y. Wu<sup>c</sup>, Sheng-Di Lin<sup>c</sup>

<sup>a</sup> Department of Physics, National Taiwan University, Taipei 106, Taiwan

<sup>b</sup> Department of Electronic and Electrical Engineering and Sungkyunkwan University Advanced Institute of Nanotechnology, Sungkyunkwan University, Suwon 440-746, Republic of Korea

<sup>c</sup> Department of Electronics Engineering, National Chiao Tung University, Hsinchu 300, Taiwan

### ARTICLE INFO

#### Article history:

Received 25 March 2010

Accepted 28 March 2010

by A.H. MacDonald

Available online 7 April 2010

#### Keywords:

A. Quantum wells

A. Semiconductors

D. Quantum localization

### ABSTRACT

We have performed magnetoresistance measurements on a Si delta-doped GaAs single quantum well. With increasing temperature  $T$ , a crossover from negative magnetoresistance (NMR) to positive magnetoresistance (PMR) can be observed. Our experimental results suggest that such a crossover corresponds to a transition from variable range hopping regime to activated electron transport. This is also consistent with the measured non-monotonic carrier density dependence on  $T$ .

© 2010 Elsevier Ltd. All rights reserved.

### 1. Introduction

Magnetoresistance (MR) is probably one of the most studied effects in the solid state. In general, there are two types of magnetoresistance. If the measured MR decreases with increasing magnetic field  $B$ , then it is called negative magnetoresistance (NMR). On the other hand, by positive magnetoresistance (PMR), we mean that the measured MR increases with increasing  $B$ . Both NMR and PMR reflect a wide variety of interesting physical phenomena. In the weakly localized (WL) regime [1], NMR occurs as time-reversal symmetry is broken. In this case, coherent backscattering effects are suppressed, leading to a decrease in the measured MR with increasing  $B$ . In the strongly localized (SL) regime, the conduction is dominated by the variable range hopping (VRH) process. The characteristic temperature dependence of hopping conduction can be described by

$$\rho_{xx}(T) = \rho_0 \exp \left[ \left( \frac{T_0}{T} \right)^p \right], \quad (1)$$

where  $p = \frac{1}{3}$  for Mott VRH [2] and  $p = \frac{1}{2}$  for Efro–Shklovskii (ES) VRH [3],  $T$ ,  $\rho_0$  and  $T_0$  are temperature, characteristic resistivity and characteristic temperature, respectively. Generally, there are

two types of theoretical model which can be used to describe the observed NMR in the SL regime [4]. The first one is due to the suppression of the destructive interference between the different hopping paths under a perpendicular magnetic field [5]. The other one is based on the density of states at the Fermi surface in  $B$ , which is called the incoherent mechanism model [6]. At strong enough magnetic fields, the dependence of hopping conductivity on  $B$  is caused by the shrinkage of the wave functions of the localized electronic states. This shrinkage leads to the decrease of the probability of the hop and therefore gives rise to PMR [3].

Delta-doped structures have been attracting much interest because of their potential device applications in electronic memory circuits [7] and in field-effect transistors [8]. Moreover, it has been demonstrated that delta-doped structures [9] are ideal systems for studying the  $B$ -induced insulator–quantum Hall transition [10–15], one of the most interesting effects in the field of two-dimensional physics. In this communication, we present magnetotransport measurements on a Si delta-doped GaAs single quantum well system. We show that a crossover from NMR to PMR can occur with increasing temperature. Interestingly, this crossover corresponds to a transition from a VRH transport regime to an activated transport regime. The measured carrier density  $n$  shows a non-monotonic  $T$  dependence. In the VRH regime,  $n$  decreases with increasing  $T$ . In the activated transport regime, the thermal energy is enough to excite electrons to the conduction band, leading to an increase in  $n$  with increasing  $T$ . The temperature where NMR completely diminishes is close

\* Corresponding author. Tel.: +886 2 23639984; fax: +886 2 23697238.  
E-mail address: [ctliang@phys.ntu.edu.tw](mailto:ctliang@phys.ntu.edu.tw) (C.-T. Liang).

to that where the carrier concentration begins to increase with increasing  $T$ .

## 2. Experimental

A Si delta-doped single GaAs quantum well structure grown by molecular beam epitaxy (MBE) was used in our experiment. The following layer sequence was grown on a semi-insulating GaAs (100) substrate: 200 nm GaAs buffer layer, 80 nm  $\text{Al}_{0.33}\text{Ga}_{0.67}\text{As}$ , 10 nm undoped GaAs, Si delta-doping with a density of  $5 \times 10^{11} \text{ cm}^{-2}$ , 10 nm undoped GaAs, 60 nm  $\text{Al}_{0.33}\text{Ga}_{0.67}\text{As}$ , and finally 10 nm doped GaAs with a concentration of  $2 \times 10^{18} \text{ cm}^{-3}$ . The top GaAs layer is doped so as to compensate surface depletion effects as normally found in a delta-doped quantum well sample [9]. We find that the doped GaAs top layer itself does not conduct over the whole temperature range. The magnetoresistivity measurements were performed in a top-loading He3 system equipped with a superconducting magnet. For  $T < 30 \text{ K}$ , the four-terminal current–voltage ( $I$ – $V$ ) characteristics of our device are highly non-linear [16]. A possible reason is that, at low  $T$ , our sample behaves as a true insulator with an immeasurably large resistance. In order to compare the observed MR, we concentrate on the results for  $T \geq 30 \text{ K}$  where linear  $I$ – $V$  curves are observed.

## 3. Results and discussion

Fig. 1 shows longitudinal resistivity  $\rho_{xx}$  measurements as a function of temperature  $T$ . We can see that our device behaves as an insulator in the sense that  $\rho_{xx}$  decreases with increasing  $T$  [12]. Over the whole measurement range, the resistivity of our device is much bigger than the resistance quantum  $\frac{h}{e^2}$ , suggesting that our sample is in the SL regime. The inset to Fig. 1 shows four-terminal  $I$ – $V$  characteristics at different  $T$ . The  $I$ – $V$  characteristics at low  $T$  are highly non-linear. We note that, at  $T = 30 \text{ K}$ , the  $I$ – $V$  curve is linear, allowing us to define the resistance of our device. We therefore concentrate on the results obtained for  $T \geq 30 \text{ K}$ .

Fig. 2 shows  $\rho_{xx}(B) - \rho_{xx}(B=0) - 1$  as a function of magnetic field at various temperatures. Over the whole measurement range,  $\rho_{xx}(B)$  decreases with increasing  $T$ . Again, our device behaves as an insulator in the sense that  $\rho_{xx}$  decreases with increasing  $T$  [12]. For  $T = 30 \text{ K}$  and  $T = 40 \text{ K}$ , pronounced NMR centered at around  $B = 0$  can be observed.

We now turn to our main experimental results. As shown in Fig. 2, with increasing  $T$ , a crossover from NMR to PMR [17] occurs between  $T = 40 \text{ K}$  and  $T = 50 \text{ K}$ . In order to further study this crossover effect, we plot logarithmic of the zero-field  $\rho_{xx}$  as a function of  $T^{\frac{1}{3}}$  in Fig. 3. In the top inset to Fig. 3, we plot the logarithm of the zero-field  $\rho_{xx}$  as a function of  $T^{\frac{1}{2}}$ . Whilst both fits are good, it is not possible for us to tell whether Mott VRH or ES VRH is the dominant mechanism in our system. Nevertheless, interestingly for  $T > 41 \text{ K}$ , deviation from either the  $T^{\frac{1}{3}}$  or the  $T^{\frac{1}{2}}$  dependence can be seen. Note that this temperature is approximately when the NMR/PMR crossover occurs. According to our data, once  $T$  is higher than 41 K, VRH is no longer the dominant transport mechanism. Therefore NMR is suppressed. In turn, PMR is observed in our system.

For  $41 \text{ K} \leq T \leq 48 \text{ K}$ , it may be possible that nearest-neighbor hopping is the dominant mechanism. As shown in the bottom inset to Fig. 3, for  $T > 48 \text{ K}$ , the data is best described by activation behaviour. From the fit, we note that the activation energy is about 11 meV. This value is substantially larger than the typical activated energy (a few meV) for nearest-neighbor hopping [17–19], so the activation behavior observed in our results can be ascribed to the excitation of carriers from localized states to extended states above the conduction band edge.

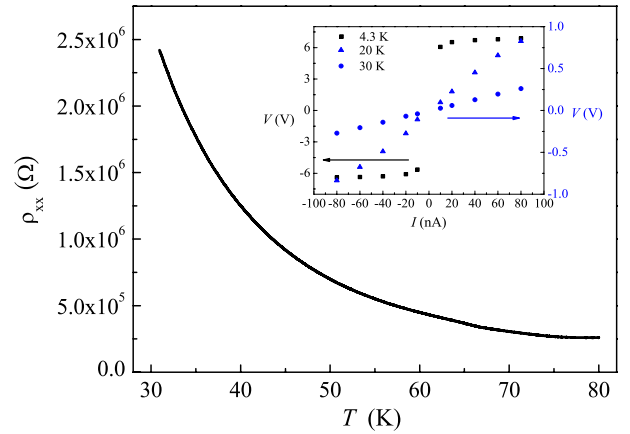


Fig. 1. Longitudinal resistivity  $\rho_{xx}$  as a function of temperature  $T$ . The inset shows the four-terminal  $I$ – $V$  at different  $T$ .

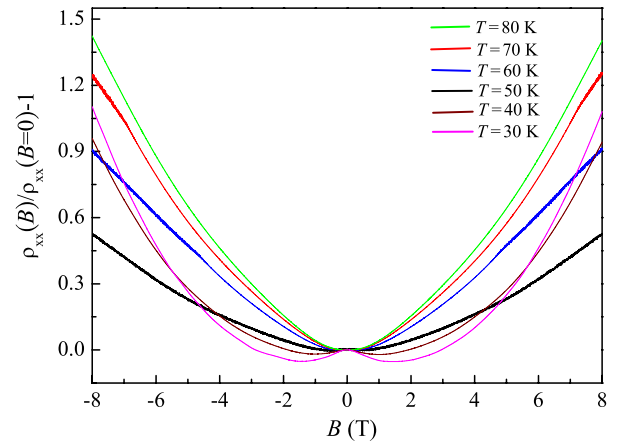


Fig. 2.  $\rho_{xx}(B)/\rho_{xx}(B=0) - 1$  at various temperatures  $T$ .

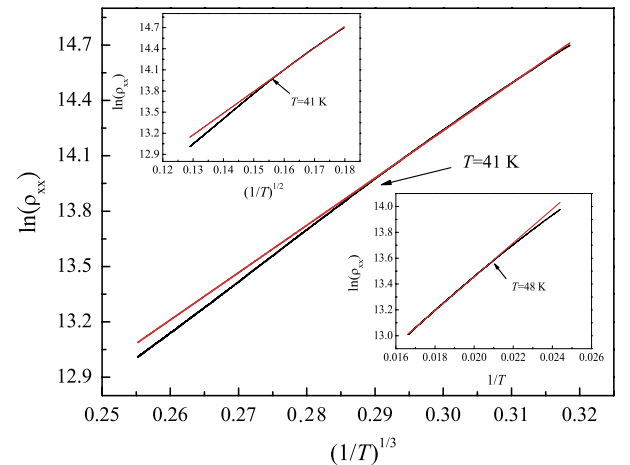
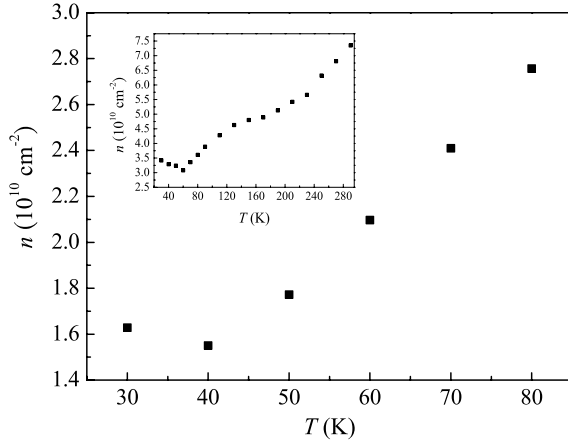


Fig. 3. Logarithm of the zero-field longitudinal resistivity  $\rho_{xx}$  as a function of  $T^{\frac{1}{3}}$ . The top inset shows  $\rho_{xx}$  as a function of  $T^{\frac{1}{2}}$ . The bottom inset shows  $\rho_{xx}$  as a function of  $\frac{1}{T}$ .

It has been suggested that measurements of the carrier density at various temperatures may reveal useful information such as a possible transition from conduction band transport to impurity band transport [20]. To this end, we have performed low-field Hall measurements to determine the carrier density  $n$  at various  $T$ . Fig. 4 shows the measured  $n$  at different  $T$ . We can see that  $n$  shows a non-monotonic dependence on  $T$ . In the VRH regime,



**Fig. 4.** The carrier concentration obtained from the low-field Hall measurements at various temperatures performed in a top-loading He3 system. Inset: Subsequent cool down in a closed-cycle system equipped with a water-cooled electric magnet.

$n$  decreases with increasing  $T$ . In the activated transport regime, the thermal energy is enough to excite electrons to the conduction band, leading to an increase in  $n$  with increasing  $T$ . Similar results are reproduced in a subsequent cool down in a closed-cycle system equipped with a water-cooled electric magnet as shown in the inset to Fig. 4. The difference between two experiments can be ascribed to different cool down conditions. As shown in Fig. 4,  $n$  starts to increase at around  $T = 40$  K. This is close to the temperature at which the crossover from NMR to PMR occurs. The observed decrease in  $n$  in the low-temperature regime can be qualitatively demonstrated by the following equation:

$$n = \frac{1}{eR} = \frac{(\sigma_1 + \sigma_2)^2}{e(R_1\sigma_1^2 + R_2\sigma_2^2)} = \frac{(\sigma_1 + \sigma_2)^2}{e(R_1\sigma_1^2)}, \quad (2)$$

where  $n$  and  $R$  denote the carrier density and the Hall slope, respectively. The subscripts 1 and 2 refer to the measurable transport quantities of activated and hopping conduction, respectively. It is assumed that  $R_2 = 0$  since  $R_2$  is too small to be measured when hopping conduction ( $\sigma_2$ ) dominates [21]. The hopping transport competes with the activated one as the temperature is lowered. It is obvious from Eq. (1) that the conventional relationship between the carrier density and the Hall slope can be obtained when the hopping conductivity  $\sigma_2$  approaches zero with increasing  $T$ . In the VRH regime,  $\sigma_2$  decreases with increasing  $T$ , leading to a decrease of  $n$  with increasing  $T$ . Therefore our results of magnetotransport measurements provide a piece of evidence that the non-monotonic  $T$  dependence of the carrier concentration is indeed due to the fact the hopping conduction should be taken into account when the Hall data is analyzed in the strongly disordered system.

Finally we address the issues of NMR at low  $B$  and PMR at high  $B$  at the two lowest  $T$  in our case. As shown in Fig. 5(a) and (b),  $\rho_{xx}$  shows a linear  $B$  dependence. For very low  $B$ , a clear  $B^2$  dependence is seen in both the top insets to Fig. 5(a) and (b). Such  $B$  dependences are consistent with quantum interference models in the SL regime [22]. In the high-field limit,  $\ln \rho_{xx}$  shows a  $B^2$  dependence, demonstrating that the observed PMR is indeed in the SL regime.

#### 4. Conclusion

In conclusion, we have observed a crossover from negative to positive magnetoresistance with increasing temperature. It is generally believed that NMR can be observed in the SL regime and the characteristic temperature dependence is described by the VRH formula. VRH conduction is the dominant transport

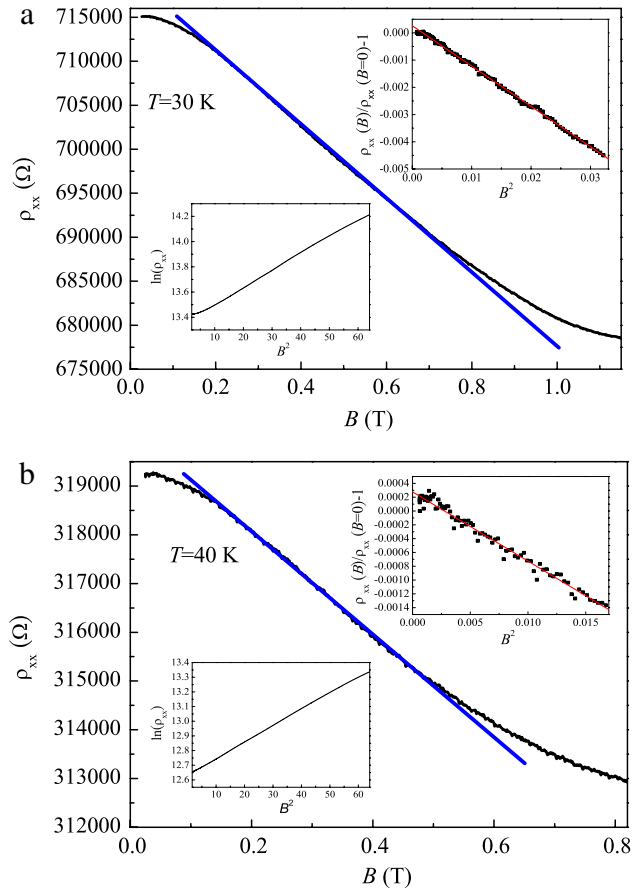


**Fig. 5.** Longitudinal resistivity as a function of the magnetic field. The quadratic magnetic-field dependence of the longitudinal resistivity can be seen in the top inset. The bottom inset shows  $\ln \rho_{xx}$  as a function of  $B^2$  at high  $B$ . The measurement temperatures are (a)  $T = 30$  K and (b)  $T = 40$  K, respectively.

process at low  $T$ , which would lead to a decrease of carrier density with increasing  $T$ . Electrons trapped by the impurities below the conduction band edge would be excited to the impurity levels where VRH is conducting, so the NMR would diminish ultimately with increasing  $T$ . A crossover from negative to positive magnetoresistance represents a transition from VRH to activated conduction.

#### Acknowledgement

This research was supported by the Basic Science Research Program through the National Research Foundation of Korea (NRF) funded by the Ministry of Education, Science and Technology (ROA-2007-000-10032-0). S.T.L. acknowledges financial support from the NSC, Taiwan (NSC 98-2815-C-002-043-M). C.T.L. thanks the NSC, Taiwan for financial support.

#### References

- [1] B.L. Altshuler, D. Khmel'nitzkii, A.I. Larkin, P.A. Lee, Phys. Rev. B 22 (1980) 5142.
- [2] N.F. Mott, E.A. Davis, Electronic Processes in Non-Crystalline Materials, Clarendon, Oxford, 1979.
- [3] B.I. Shklovskii, A.L. Efros, Electronic Properties of Doped Semiconductors, in: Springer Series in Solid-State Sciences, vol. 45, Springer, Berlin, 1984.
- [4] H.W. Jiang, C.E. Johnson, K.L. Wang, Phys. Rev. B 46 (1992) 12830.
- [5] V.L. Nguyen, B.Z. Spivak, B.I. Shklovskii, JETP Lett. 41 (1985) 42.
- [6] M.E. Raikh, Solid State Commun. 75 (1990) 935.
- [7] K. Nakazato, R.J. Blaikie, H. Ahmed, J. Appl. Phys. 75 (1994) 5123.
- [8] E.F. Schubert, A. Fischer, K. Ploog, IEEE Trans. Electron Devices 33 (1986) 625.

- [9] C.H. Lee, Y.H. Chang, Y.W. Suen, H.H. Lin, *Phys. Rev. B* 58 (1998) 10629.
- [10] S. Kivelson, D.H. Lee, S.C. Zhang, *Phys. Rev. B* 46 (1992) 2223.
- [11] H.W. Jiang, C.E. Johnson, K.L. Wang, S.T. Hannahs, *Phys. Rev. Lett.* 71 (1993) 1439.
- [12] S.-H. Song, D. Shahar, D.C. Tsui, Y.H. Xie, D. Monroe, *Phys. Rev. Lett.* 78 (1997) 2200.
- [13] C.F. Huang, Y.H. Chang, C.H. Lee, H.T. Chou, H.D. Yeh, C.-T. Liang, Y.F. Chen, H.H. Lin, H.H. Cheng, G.J. Hwang, *Phys. Rev. B* 65 (2002) 045303.
- [14] G.-H. Kim, C.-T. Liang, C.F. Huang, J.T. Nicholls, D.A. Ritchie, P.S. Kim, C.H. Oh, J.R. Juang, Y.H. Chang, *Phys. Rev. B* 69 (2004) 073311.
- [15] T.-Y. Huang, C.-T. Liang, G.-H. Kim, C.F. Huang, C.P. Huang, J.-Y. Lin, H.S. Goan, D.A. Ritchie, *Phys. Rev. B* 78 (2008) 113305.
- [16] D.P. Wang, D.E. Feldman, B.R. Perkins, A.J. Yin, G.H. Wang, J.M. Xua, A. Zaslavsky, *Solid State Commun.* 142 (2007) 287.
- [17] A.V. Buyanov, A.C. Ferreira, E. Soderstrom, I.A. Buyanova, P.O. Holtz, B. Sernelius, B. Monemar, M. Sundaram, K. Campman, J.L. Merz, A.C. Gossard, *Phys. Rev. B* 53 (1996) 1357.
- [18] Q. Ye, B.I. Shklovskii, A. Zrenner, F. Koch, K. Ploog, *Phys. Rev. B* 41 (1990) 8477.
- [19] E.I. Levin, M.E. Raikh, B.I. Shklovskii, *Phys. Rev. B* 44 (1991) 11281.
- [20] A. Yildiz, S.B. Lisesivdin, H. Altuntas, M. Kasap, S. Ozelik, *Physica B* 404 (2009) 4202.
- [21] D.C. Look, D.C. Walters, M.O. Manasreh, J.R. Sizelove, C.E. Stutz, K.R. Evans, *Phys. Rev. B* 42 (1990) 3578.
- [22] M.E. Raikh, G.F. Wessels, *Phys. Rev. B* 47 (1993) 15609.